ELSEVIER

Chemical Engineering Science 60 (2005) 5544–5554

Chemical Engineering Science

www.elsevier.com/locate/ces

An arrangement of ideal zones with shifting boundaries as a way to model mixing processes in unsteady stirring conditions in agitated vessels

J.-Y. Dieulot[a,*], N. Petit[b], P. Rouchon[b], G. Delaplace[c]

[a]*L.A.G.I.S., Laboratoire d'Automatique Génie Informatique et Signal, UMR CNRS 8146, I.A.A.L Ecole Polytechnique Universitaire de Lille, 59655 Villeneuve d'Ascq-France*

[b]*Centre Automatique et Systèmes, École des Mines de Paris, 60 Boulevard Saint Michel, 75272 Paris Cedex 06, France*

[c]*I.N.R.A. Institut National de la Recherche Agronomique, Laboratory for food Process Engineering and Technology, 369, rue Jules Guesde, B.P. 39, 59651 Villeneuve d'Ascq-France*

Received 19 July 2004; received in revised form 2 March 2005; accepted 2 March 2005
Available online 28 June 2005

Abstract

This paper investigates the way modelling mixing phenomena occur in unsteady stirring conditions in agitated vessels. In particular, a new model of torus reactor including a well-mixed zone and a transport zone is proposed. The originality of the arrangement of ideal reactors developed here lies in the time-dependent location of the boundaries between the two zones. This concept is applied to model the positive influence of unsteady stirring conditions on homogenization process: the model avoids a mass balance discontinuity when the transition from steady to unsteady stirring conditions is performed.

To ascertain the reliability of the model proposed, experimental runs with highly viscous fluids have been carried out in an agitated tank. The impeller used was a non-standard helical ribbon impeller, fitted with an anchor at the bottom. The degree of homogeneity in the tank was observed using a conductivity method after a tracer injection.

It is shown that for a given agitated fluid and mixing system, model parameters are easy to estimate and that modelling results are in close agreement with experimental ones. Moreover, it would appear that this model allows the easy derivation of a control law, which is a great advantage when optimizing the dynamics of a mixing process.

Keywords: Mixing; Modelling; Nonlinear dynamics; Parameter identification; Unsteady stirring; Torus model

1. Introduction

1.1. Enhancement of mixing with unsteady flows

High viscosity mixing operations in agitated vessels are commonly encountered in chemical and food industries. Since batch mixing operations are both time and energy consuming, their optimization remains an important challenge. Depending on whether the design of the mixing system is set or not, there are various possible ways to improve mixing:

- The first one is to select, for a given mixing system, the geometrical parameters (wall-clearance, shape of the bottom, bottom clearance, number of baffles) which optimize the overall homogenization efficiency. Of course, this has already been largely covered in the literature. For example, one may mention papers concerning the determination of power consumption and mixing times, under steady rotational speeds, for mixing systems equipped with close clearance impellers such as screw or helical ribbon agitators (Tatterson, 1994; Delaplace et al., 2000a), which are known to be the best suited to achieve mixing of highly viscous media.

* Corresponding author. Tel.: +33 3 28 76 74 95; fax: +33 3 28 76 74 01.
E-mail addresses: jean-yves.dieulot@polytech-lille.fr (J.-Y. Dieulot), delapla@lille.inra.fr (G. Delaplace).

0009-2509/$ - see front matter © 2005 Elsevier Ltd. All rights reserved.
doi:10.1016/j.ces.2005.03.067

- The second way is to consider that, for a given mixing system, the ability of a flow to homogenize viscous products can be significantly enhanced with the help of unsteady time-varying stirring approaches. Efficient mixing in laminar regime has been shown to be related to the amount of stretching and folding generated within the tank by the agitator (Ottino, 1989; De La Villeon et al., 1998; Alvarez-Hernández et al., 2002). When stirring conditions are steady, initially designated fluid material will follow closed streamlines in the vessel and consequently the mixing efficiency will be rather poor since such regular flows will induce a linear evolution of intermaterial area with time (Niederkorn and Ottino, 1994). However, when a suitable perturbation is superimposed on the steady velocity field, flows reorientations will appear, fluid elements will be no longer trapped by closed steady streamlines and will become free to wander throughout chaotic flow domains. As the stretching rate is higher in these flow regions, the inter-material area will grow faster (Niederkorn and Ottino, 1994; Alvarez-Hernández et al., 2002) and higher than average values of the efficiency will be obtained.

However, there is a lack of systematic studies that provide us with quantitative information about the conditions under which these chaotic flows are produced within a stirred tank and their actual benefits on mixing efficiency. Consequently, the design of a sequence of flows which involves a reorientation of material elements (for instance, when periodic or co-reverse rotation of the impeller is performed) has yet to be clearly identified.

Moreover, most unsteady stirring approaches used to improve laminar mixing in batch reactors (Nomura et al., 1997; Lamberto et al., 1996; Yao et al., 1998) deal with small-diameter agitators which are usually devoted to work in turbulent regime and not suited for the batch mixing of viscous fluids; their purpose being to prevent the formation of isolated mixed regions (Metzner and Taylor, 1960) with co-reverse or periodic rotational speed sequences. Such a work has not been carried out for systems equipped with efficient closed-clearance impellers.

1.2. Flow modelling in batch reactors

From this survey, it would appear clearly that there is a strong need for rational studies which quantify the efficiency of a stretching process for a given mixing system under unsteady operating conditions. Numerical studies using computational fluid dynamics (CFD) methods allow the determination of the whole velocity field for laminar mixing within the tank at steady and unsteady rotational speeds and thus point out the well-mixed and stagnant zones (e.g. Zalc et al., 2002; Arratia et al., 2004; Harvey and Rogers, 1996; Campolo et al., 2003). However, these finite element methods require a long computation time (e.g. for a vessel with close clearance impeller, see de la Villeon et al., 1998 for details). With these models, one cannot extrapolate the behaviour of the mixing device for a new rotational speed sequence, and no quantitative indication is given as to what rotational speed pattern should be used to optimize mixing (Alvarez-Hernández, et al., 2002). Consequently, one cannot design an optimal control that minimizes energy or time expense to achieve a given degree of homogeneity.

It is, therefore, essential to design a proper and simplified flow model for such mixing processes, incorporating the significant features of partially chaotic phenomena and usable to assess the combined effects of unsteady and steady stirring approaches on mixing efficiency, thereby allowing fast prediction and eventually the derivation of a control law.

Networks of ideal reactors have been used since the 1960s to model mixing with steady stirring approaches. Khang and Levenspiel's (1976) model consists of a plug flow reactor in series with a single continuous stirred tank reactor, with total recycling, in which the fluid flows with a constant flow rate $\dot{Q}$. Assuming that both the volume of these two ideal reactors (V_p for the plug flow reactor and V_d for the well mixed zone) are constant and that the flow rate $\dot{Q}$ which appears in the model is proportional to the rotational speed of the impeller N, it was possible by one experimental run (one tracer injection) to determine the space–time parameters of each ideal mixers (time delay θ for a plug flow reactor $\theta = V_p/\dot{Q}$ and mean residence time $T = V_d/\dot{Q}$ for a CSTR).

This simple model has now been extended (Dieulot et al., 2002) to unsteady mixing, along with an additional CSTR in the recycle loop which represents the benefit (due to additional stretching) of mixing at an unsteady rotational speed which was observed experimentally. As has been previously discussed (Dieulot et al., 2002), this model allows us to use the same network of ideal mixers to simulate the mixing performances of the agitated vessel for both the steady and unsteady approaches. The model allows fast prediction and involves only three geometrical parameters that can be easily determined from only two experimental runs (one at constant impeller speed and the two others using unsteady rotational speed experiments). However, the extension to unsteady flow is not straightforward: the expression of the time delay in the plug flow zone is complicated and, moreover, the introduction of the additional volume does not allow the mass balance to be respected.

This has been the motivation for the model presented in the next section. In order to respect the mass balance, the decision was taken to add no further ideal reactors (as the additional CSTR in the previous study) to account for changes in mixing conditions when transition from steady to unsteady stirring approaches is carried out. On the contrary, an attempt was carried out to model the increase in mixing efficiency due to unsteady stirring conditions both by adapting the relative volume ratios of the ideal zones which compose the final model and by keeping the volume of each ideal zone unchanged. This was achieved by using a juxtaposition of a plug flow zone and a well-mixed zone contained in a torus volume with time varying boundaries. In the

following section, we will give more details about the basis of the model and mathematical expressions of the space–time parameters for the ideal reactors contained in the torus volume. Experimental mixing runs (for steady and unsteady stirring approaches) were used to ascertain the validity and to compare performances of this model with those found in the literature. Note that the ultimate framework of this scientific programme is to determine an optimal controller, i.e., the rotational speed profile that minimizes the mixing energy for a given mixing time.

2. Principle of the torus reactor model

Consider a torus of fixed volume V divided into two ideal reactors (a constant stirred tank reactor of volume V_d and a plug flow zone of volume $V_p = V - V_d$) in which flows a Newtonian fluid with a uniform time-varying flow rate $\dot{Q}$ in a clockwise direction (Fig. 1). $y(t)$ refers to the fluid concentration (kg/m^3) in component y (tracer) which varies with time and space. It is assumed that the total material quantity of the component y in the reactor remains constant.

The originality of the torus reactor arises from the time-dependent position of the boundaries (S_1 and S_2) which separate the two ideal flow zones. Indeed, it is assumed that S_1 and S_2 move alternately in a counter-clockwise direction to the flow rate fluctuations. Consequently, when the flow rate is non-steady, the volumes (V_d and V_p) of the two ideal reactors are time variant. In particular, it is assumed that S_1 (respectively, S_2) move only when positive (respectively, negative) variations in the flow rate occur in the torus volume and is otherwise motionless. Note also, that when a variation of flow rate occurs, not only the volume of the zones vary but their location within the torus evolves counter-clockwise.

Assuming that at each time t the flow rate $\dot{Q}(t)$ is proportional to the impeller rotational speed $N(t)$ (via α (m^3), a constant: $\dot{Q}(t) = \alpha N(t)$), the torus model proposed is likely

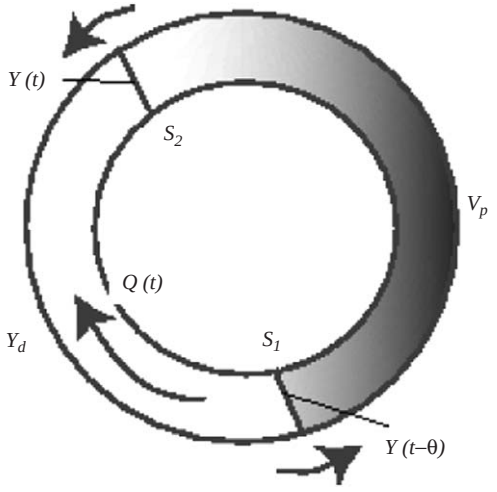

Fig. 1. Sketch of torus model proposed in this study.

to describe the response curve after a tracer injection, whatever the stirring approach adopted. Indeed, for steady approaches the network of ideal mixers used to simulate the mixing process becomes similar to that of those used by Khang and Levenspiel (1976) whose reliability have been previously shown. Moreover, in the case of unsteady stirring, the model is also supposed to account for the experimental observation that an improvement in mixing occurs when a positive variation in the rotational speed is enforced. For example, in the case of a positive variation in impeller rotational speed, the volume of the stirred tank reactor increases while that of the plug flow decreases. As the whole volume of the torus loop is supposed to be unchanged, an enhancement in mixing is expected.

Note that the model structure should not be confused with real toroidal reactors (e.g. Benkhelifa et al., 2000).

Let us define $\dot{V}_d^+$ (resp., $\dot{V}_d^-$) as the variation of volume V_d due to the motion of S_1 (resp., S_2) in the torus, and let θ be the residence time of the particle leaving the plug flow zone at time t. Using notations previously introduced, the whole system can be characterized by the following differential equations (see Appendix A):

$$\begin{aligned} &V = V_d(t) + V_p(t),\\ &\int_{t-\theta}^{t} \dot{Q}(\sigma)\,\mathrm{d}\sigma = V - V_d(\dot{Q}(t-\theta)) - \int_{t-\theta}^{t} \dot{V}_d^+(\sigma)\,\mathrm{d}\sigma,\\ &V_d(\dot{Q}(t))\frac{\mathrm{d}[y(t)]}{\mathrm{d}t} = (\dot{Q}(t) + \dot{V}_d^+)[y(t-\theta) - y(t)],\\ &\dot{Q}(t) = \alpha N(t). \end{aligned} \tag{1}$$

2.1. Theorem

The mass balance in the species $y(t)$ within the torus reactor defined by Eq. (1) is respected (see proof in Appendix B).

In our study, it is assumed that in the case of steady mixing (constant rotational speed), the volume of the well-mixed zone does not depend on the amplitude of the rotational speed and has a constant value V_{d_1}. Note that integrating Eq. (1), we obtain

$$V_d(t) = \int_0^t \dot{V}_d^+\,\mathrm{d}t - \int_0^t \dot{V}_d^-\,\mathrm{d}t + V_{d_1}, \tag{2}$$

where V_{d_1} is the initial volume of the well-stirred zone.

Assuming that the total volume of torus reactor V corresponds to the volume of the agitated fluid, the proposed system involves five unknown variables or parameters α, V_{d_1}, $\dot{V}_d^+(t)$, $\dot{V}_d^-(t)$ and $y(t)$.

Providing two prerequisites, a simulation algorithm can be used to predict the output $y(t)$:

- the two constant parameters (α and V_{d_1}), which are not influenced by the time-dependent rotational speed, are known.
- the effects of stirring conditions $N(t)$ on boundary motions (S_1 and S_2) are established. Indeed, such knowledge

will allow $\dot{V}_d^+$ and $\dot{V}_d^-$ to be obtained at each time. Consequently, V_d and V_p can also be computed.

The assumptions used in this paper concerning evolutions of $\dot{V}_d^+$ and $\dot{V}_d^-$ with stirring conditions are the following, which requires a third constant parameter k for the model:

$$\dot{V}_d^+ = k\frac{\mathrm{d}N}{\mathrm{d}t} \text{ if } \frac{\mathrm{d}N}{\mathrm{d}t} > 0, \quad \dot{V}_d^+ = 0 \text{ if } \frac{\mathrm{d}N}{\mathrm{d}t} < 0,$$
$$\dot{V}_d^- = -k\frac{\mathrm{d}N}{\mathrm{d}t} \text{ if } \frac{\mathrm{d}N}{\mathrm{d}t} < 0, \quad \dot{V}_d^- = 0 \text{ if } \frac{\mathrm{d}N}{\mathrm{d}t} > 0. \qquad (3)$$

The simulation of a system involving an input-dependent transport delay is not always trivial, since the delay is defined by an implicit equation. In particular, Zenger and Ylinen (1994) have shown that for most flow rate fluctuations, the expression of $\theta(t)$ cannot be obtained analytically but must be computed by numerical methods. In this work, for the sake of simplicity, it has been chosen not to deal with this issue in detail. More information about the computational methods used in this work can be found in the original publication (Zenger and Ylinen, 1994) or in a previous paper (Dieulot et al., 2002).

Finally, note that the simulation algorithm has been developed considering the torus model as a discrete automaton. First, the torus has been divided into a large number of cells. At each simulation step, the values of the concentration should move from one cell of the plug flow zone to the next one, using the definition of a plug flow reactor (pure transport). The concentration in the well-mixed zone can then be computed using a total mass balance and the fact that the concentrations in each cell of the zone are equal. The boundaries are then updated. The time step is variable and corresponds to the residence time in a cell, which depends on the flow rate values (rotational speed).

3. Material and methods

3.1. Apparatus used to monitor mixing experiments

The mixing equipment used appears in Fig. 2. During all the experiments, the level of the liquid at rest was maintained at a constant level of 0.402 m in height for a total volume of 30×10^{-3} m^3. Experiments were carried out with the helix pumping upward (counter-clockwise direction of rotation). Additional information about the flow pattern produced by the mixing system is given elsewhere (Delaplace et al., 2000a,b).

The agitated fluid is an aqueous solution of glucose with a viscosity of 1.8 Pa s at 26 °C. A controlled speed rotational viscometer (CONTRAVES, Rheomat 30) was used to determine the Newtonian viscosity of the viscous medium. The shear rate ranged from 0.1–500 s^{-1} and the dependence of viscosity and density on temperature was taken into account.

A conductivity probe (SOLEA-TACCUSSEL, type CD 78) was used to obtain the circulation curves in the vessel

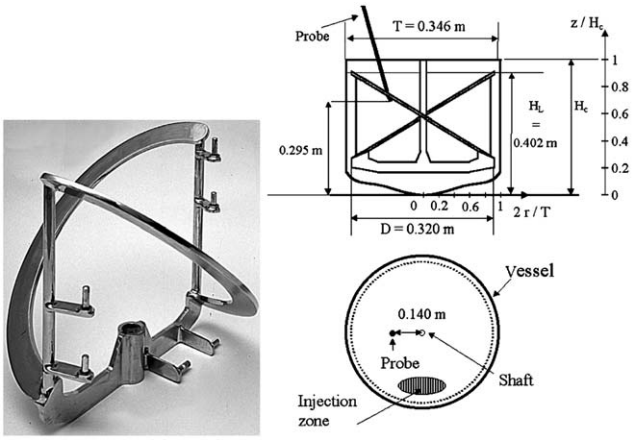

Fig. 2. Picture and geometrical parameter of the mixing equipment investigated (other geometrical parameters of PARAVISC® mixing system: blade width, $w = 0.032$ m; impeller pitch, $p = 0.560$ m; impeller height, $L = 0.340$ m; tank height, $H_c = 0.443$ m).

after a tracer injection. The signal was amplified by a converter (Type AT40, SFERE), and recorded with the help of an I/O board (PCL-812 PG, ADVANTECH) plugged into a PC. The sampling rate was 200 Hz.

The tracer pulse injected had the same physical properties as the fluid in the tank (composition and temperature), with an additional quantity of NaCl at a concentration of 100 g/l. The incorporation was performed with the help of a pneumatic system with pistons (type DACO, PCM DOSYS) equipped with a duct (DACC 48/40, DOSYS) which holds the product at the end of the pipe. This device was able to inject 72 ml (0.24% of the tank volume) of viscous tracer into the tank with an accuracy of 2%. The injection duration is by a fraction of a second. It was checked, measuring a sample of the injected fluid before and after each injection, that the influence of the addition of salt on density and viscosity was negligible for a limited (40) number of successive trials. The volume of the tank was brought back to 30×10^{-3} m^3 after each experiment. The conductivity probe and the injection locations were kept unchanged throughout the experiments (Fig. 2).

The I/O board allows the operating conditions to be accurately controlled, i.e., the injection time, the departure and the magnitude of speed variations that were enforced on the agitation system. The rotational speed and the conductivity signal were recorded throughout the mixing process. Recording was activated 3 s before the tracer injection. Each experiment (for one set of experimental conditions) was repeated four times to ensure repeatability.

The values of the rotational speed varied from 0.16 to 1.5 rev/s. Mixing and circulation times were determined from the response signal recorded after tracer injection. The mixing time is defined as the duration needed for the signal to reach 95% of its final value (Fig. 3). The circulation time is defined as the signal period, when mixing at constant impeller rotational speed (Fig. 3). When the conductivity

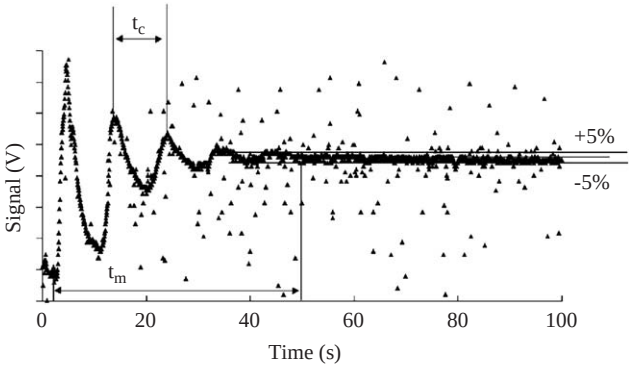

Fig. 3. A typical probe response curve.

method was used, it is clear that the values of circulation and mixing times depend significantly on the location of the injection point and measurement probe. Nevertheless, for the experimental conditions tested, the local values of axial circulation times obtained are in close agreement with the global values obtained by following the movement of freely suspended particles. Moreover, global values of axial circulation times deduced from CFD velocity field (Delaplace et al., 2000a) were also in close agreement with those obtained by the conductivity method.

The conductivity signals (axial circulation curves) were particularly noisy, owing to recording problems and high-frequency environmental noise (Fig. 3). Filtering consisted, firstly, in the elimination of scatters. Measuring points with a derivative higher than a threshold value (empirically five times the signal derivative standard deviation) were replaced by an average value of their neighbours. The sampling period selected was 1 s. This choice was important for parametric identification and has been already justified and discussed elsewhere (Dieulot et al., 2002).

3.2. Operating stirring conditions tested

Table 1 shows the different types of operating stirring conditions tested after tracer injection. Trials (1) and (2) refer to well-known steady stirring approaches, whereas trials (3) to (8) concern unsteady stirring approaches. In the context of this paper, trials (3) to (4) will be called “speed ramps”, trials (5) to (7) “speed pulses” and trial (8) “speed step”.

Note that for each type of perturbation, different operating conditions were adopted (e.g. various lapses of time between tracer injection and the start of the impeller rotational speed fluctuations (PS)). The various operating conditions tested are also reported in Table 1.

3.3. Parameter identification: V_{d_1}, α, k

The torus model proposed requires the estimation of three constant parameters V_{d_1}, α, k (defined by Eqs. (1)–(3)), which depend on the characteristics of the mixing device and on the viscous media (which are maintained at a constant level in this study).

Parameters V_{d_1} and α have been estimated from one tracer experiment when mixing at constant impeller speed (0.667 rev/s—trial number 1 in Table 1). Using the values of the parameters V_{d_1} and α previously estimated, an additional injection was performed with unsteady stirring conditions (a speed pulse—trial number five in Table 1) to obtain the value of parameter k.

The set of model parameters were estimated using an optimization algorithm (simplex method). The optimization algorithm is based on the minimization of the mean absolute error criterion defined in Eq. (4).

$$\mathrm{MAE} = \frac{1}{M} \sum_{i=0}^{M-1} |\varepsilon(i.T_e)|. \tag{4}$$

This criterion represents the sum of the absolute differences, $|\varepsilon(i.T_e)|$, between the experimental points and the estimated points, T_e is the sampling period (1 s) and M is the number of samples required to describe the homogenization process. The importance of this criterion was discussed by Dieulot et al. (2002), where it was shown that it leads to a good compromise between minimizing the shifting between real and modelling curves (due to time delay estimation mismatch) and other errors due to unmodelled non-linearities.

3.4. Reliability of the model

Using different operating conditions (trials 2–4 and 6–8 in Table 2) to those adopted for parameter estimation (trials 1 and 5), the validity of the model was tested. The reliability procedure consists of comparing experimental and predicted mixing times (obtained with the help of estimated parameters). The mean absolute error between experimental and model data was also computed and its value was compared to those obtained for the trials used for fitting.

4. Results

4.1. Efficiency of mixing using unsteady stirring conditions

The positive influence of unsteady stirring condition on mixing efficiency is recalled in Table 2. It can be observed that the mixing work required for unsteady stirring is less significant than those calculated for those mixing procedures which would give identical mixing times at constant RPM. These values of energy consumed and their determinations have already been discussed (Dieulot et al., 2002) and are not the key consideration of this work. Note simply that, as presented in previous works, depending upon the type of unsteady stirring conditions adopted, the energy savings vary from 30% to 60% and justify the interest of introducing time-dependent perturbations for a homogenization process.

Table 1
Operating conditions (impeller rotational speed fluctuations) adopted during the mixing process after tracer injection

Trial number	Name and type of impeller rotational speed fluctuation		N_1 (rev/s)	N_2 (rev/s)	Time parameters (s)
1	Steady Stirring		0.667	—	—
2	Steady stirring	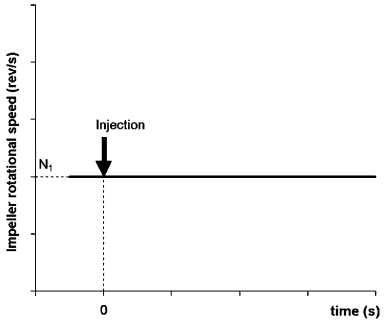	0.833	—	—
					RD
3	Ramp Speed		0.667	1.333	5
4	Ramp Speed	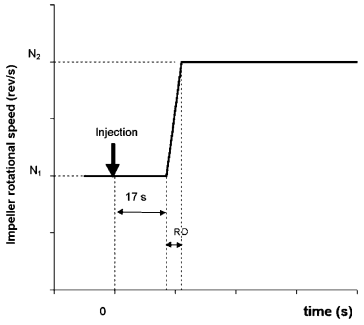	0.667	1.333	15
					PS
5	Pulse Speed		0.667	1.333	17
6	Pulse Speed		0.667	1.333	10
					4
7	Pulse Speed	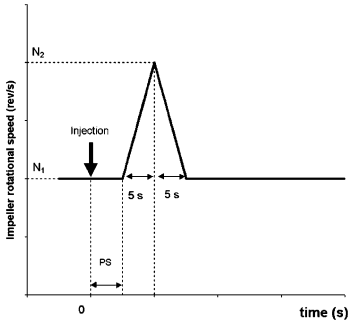	0.667	1.333	
8	Step speed	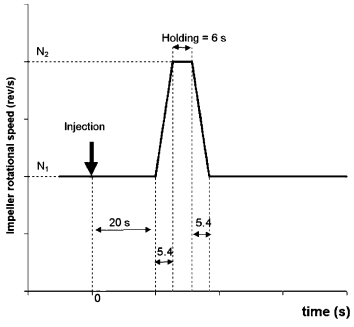	0.667	1.333	—

4.2. Validity of the model

The predictive model developed in this study has been tested on our mixing equipment. As mentioned before, one trial at constant impeller speed (trial 1) and one run at unsteady impeller speed (a pulse—trial 5—see Table 3) were necessary to determine the various ideal zone parameters. The values of the parameters estimated are $V_{d_1} =$

Table 2
Experimental mixing performances of the helical mixing system studied using various stirring conditions (starting impeller rotational speed = 0.667 rev/s except trial 2)

	Trial 1 Steady stirring	Trial 2 Steady stirring	Trial 3 Ramp (RD = 5 s)	Trial 4 Ramp (RD = 15 s)	Trial 5 Pulse (PS = 17 s)	Trial 6 Pulse (PS = 10 s)	Trial 7 Pulse (PS = 4 s)	Trial 8 Step
Experimental mixing time (s)	80.7	72	33	38.5	60.7	58.5	65.1	53.3
Experimental mixing work (J)	627.9	937.8	793.6	763.6	510.9	525.6	385	579.7
Values of mixing work (J) for the mixing process which would give same mixing time at constant impeller rotational speed[12]	627.9	937.8	1535.5	1214.3	740.4	814.6	1035.7	980.9
Energy savings	—	—	48.3	37.1	31.0	35.5	62.8	40.9

Table 3
Values of MAE and predicted values of mixing times obtained by the model for the helical mixing system studied using various stirring conditions

	Operating conditions used for parameter identification		Operating conditions used for model validation					
	Trial 1 Steady stirring $N = 0.667$ rev/s	Trial 5 Pulse (PS = 17 s)	Trial 2 Steady stirring $N = 0.833$ rev/s	Trial 3 Ramp (RD = 5 s)	Trial 4 Ramp (RD = 15 s)	Trial 6 Pulse (PS = 10 s)	Trial 7 Pulse (PS = 4 s)	Trial 8 Step
Experimental mixing time (s)	80.7	60.7	72	33	38.5	58.5	65.1	53.3
Predicted values of mixing time (s)	81.5	66.7	65.6	31.5	37.4	66.7	66.5	47.5
Values of criterion MAE (V)	0.24	0.26	0.27	0.24	0.28	0.20	0.18	0.24

$6.0\,10^{-3}\,m^3$; $\alpha = 1.61\,10^{-3}\,m^3$; $k = 4.5\,10^{-3}\,m^3\,s$ and were then used with other stirring conditions (see Table 3) to validate the proposed model.

Examples of curve fitting obtained by this approach are given in Figs. 4–9. These figures show that the estimated response curve after tracer injection is close to the experimental one, despite the high noise observed for the experimental curves and the non-linearities (such as the non-periodicity of signals which sometimes occurs at constant impeller speeds). Moreover, in order to test the accuracy of the model, the values of measured mixing times and values calculated by the model are reported in Table 3. We can note that there are close agreements between the experimental and predicted values of mixing times, whatever the stirring conditions adopted (mean error 6.8%). As previously explained, another criterion has also been computed to estimate the validity of the model: the sum of the absolute differences between the calculated and experimental outlet curves. Values of the mean absolute error (MAE) between experimental and model data are also reported in Table 3.

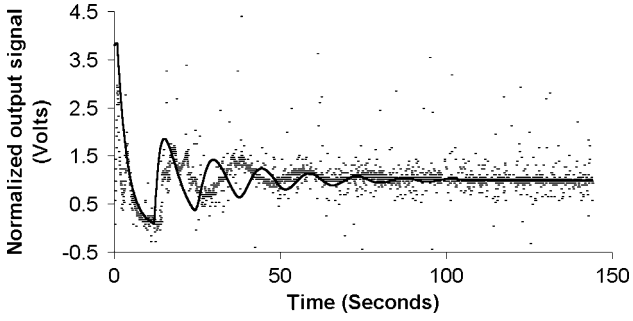

Fig. 4. Predicted (-) and experimental (.) circulation curves for steady speed at 40 rpm.

The values of MAE deduced from trials used for model validation (0.18, 0.28) are not significantly different from

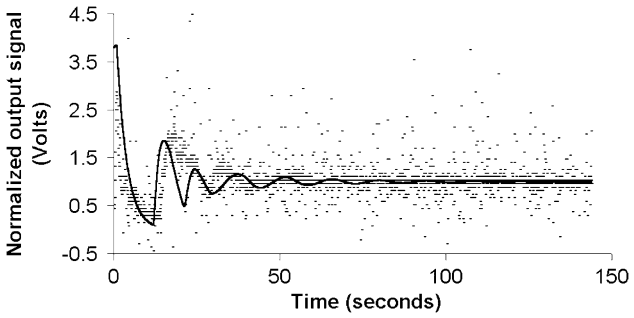

Fig. 5. Predicted (-) and experimental (.) circulation curves for speed pulse from 40 to 80 rpm, starting at 17 s, duration 5 s (trial 5 in Table 2).

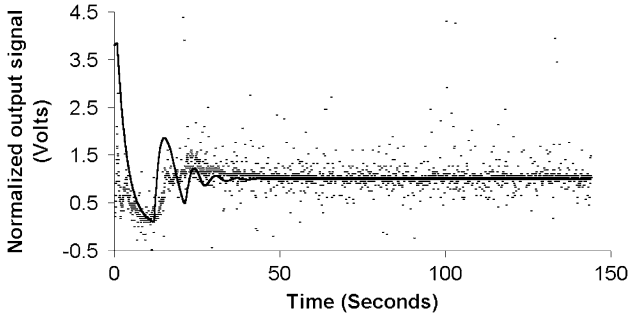

Fig. 6. Predicted (-) and experimental (.) circulation curves for speed ramp from 40 to 80 rpm, starting at 17 s, ramp duration RD = 5 s (trial 4 in Table 2).

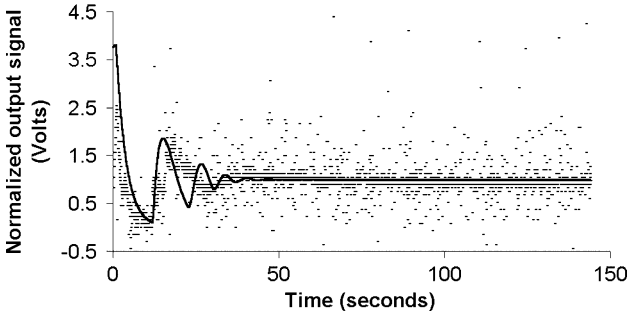

Fig. 7. Predicted (-) and experimental (.) circulation curves for speed ramp from 40 to 80 rpm, starting at 17 s, ramp duration RD = 15 s. (trial 3 in Table 2).

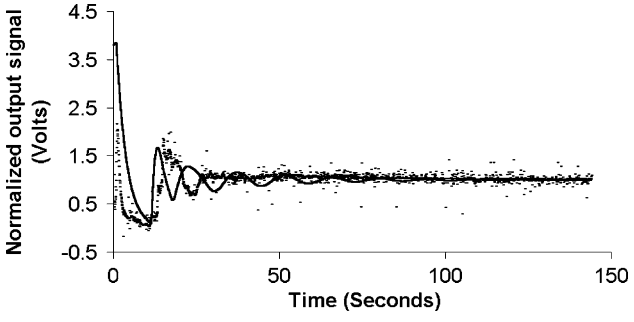

Fig. 8. Predicted (-) and experimental (.) circulation curves for speed pulse from 40 to 80 rpm, starting at 10 s, duration 5 s. PS = 10 s (trial 6 in Table 2).

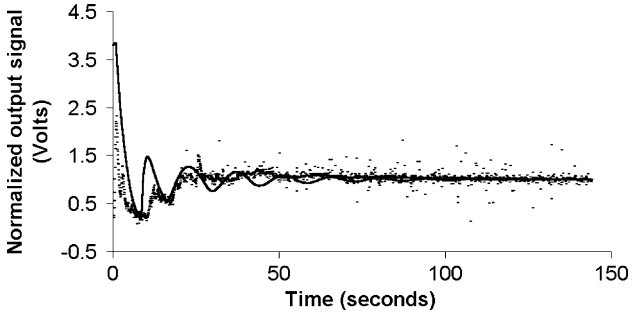

Fig. 9. Predicted (-) and experimental (.) circulation curves for speed pulse from 40 to 80 rpm, starting at 4 s, duration 5 s. PS = 4 s (trial 7 in Table 2).

those deduced from trial used for parameter estimation (0.25), and show that the model is in accordance with the experimental curves.

All these experimental results concerning modelling show us that it is possible to describe the mixing process which occurs under steady or unsteady stirring using the structure of the proposed model. It is thus possible to perform fast mixing time computations (less than 1 s on a PC) for any rotational speed profile. One major interest of the torus reactor compared to previous studies (Dieulot et al., 2002) is that the mass balance in the species within the batch reactor is respected. Note that the toroidal reactor model is not a limited concept only applied for a specific mixing system design. On the contrary, the proposed model can be generalized to describe other mixing processes at steady or unsteady rotational speeds in stirred tanks.

Another motivation to use the torus reactor relies on deriving a control law from mathematical equations (for the rotational speed of the impeller) which thereby optimizes mixing dynamics. Indeed, introducing the following change in time-scale:

$$\mathrm{d}s = (\dot{Q}(t) + \dot{V}_d^+)\,\mathrm{d}t, \tag{5}$$

the mass-balance equations become

$$s(t) - s(t-\theta) = V_p \quad \text{and} \quad V_d(U(s))\frac{\mathrm{d}Y}{\mathrm{d}s}(s) = Y(s-\varsigma) - Y(s), \tag{6}$$

where $\dot{Q} = U(s(t))$; $y(t) = Y(s(t))$ and ς is defined by $\varsigma = V_p(U(s-\varsigma))$.

From Eqs. (5) and (6), it can be seen that, if V_d is an increasing function of u, then there is a difference when $u > 0$ ($\dot{V}_d^+ \neq 0$) and $u < 0$ ($\dot{V}_d^+ = 0$), and that for $u > 0$ the new "time" $s(t)$ passes faster. Mixing is thus more efficient when the flow accelerates, which is consistent with experimental observations. This can be illustrated by considering a flow with a saw tooth profile, for which the volumes will return to their initial value after the saw tooth is completed. In a first instance, the boundary S_1 moves and V_d expands. When S_2 moves in turn and V_p expands as u decreases, the

plug flow zone will move counter-clockwise and will overlap an area which was previously in the well-mixed zone. The effect of $u<0$ is thus more limited than in the case where $u>0$.

Finally, defining ς by $W=V_d(U)$ as the control parameter and using volume balance in the torus, it can be written

$$W\frac{\mathrm{d}Y}{\mathrm{d}s}(s)=Y(s-\varsigma)-Y(s) \quad \text{and}$$
$$\varsigma+V_d(U(s-\varsigma))=V. \tag{7}$$

By construction $W\in[0,V]$ and a positive solution for ς always exists when W is a continuous function of s. When the equation has several roots, ς should be chosen as the smallest. Consequently, using the torus model, an optimal solution for the control should be quite simple to obtain using algebraic methods. Preliminary results have been obtained (Dieulot and Richard, 2001), which will be extended in future work.

5. Conclusion

A torus model has been developed to describe a mixing process at unsteady rotational speeds. The combination of ideal reactors proposed includes a well-mixed and a plug flow zone contained in a torus volume. The boundaries between the two zones vary with the flow rate (proportional to impeller rotational speed) and are supposed to represent the enhancement of mixing efficiency, experimentally observed when using unsteady stirring conditions. Only the knowledge of three constant parameters V_{d_1}, α, k is required for the model proposed. Moreover, only two trials are necessary to estimate the three fixed parameters (one at constant impeller speed V_{d_1}, α, and one at unsteady rotational speed k). Finally, the model proposed gives a close agreement between predicted and experimental circulation curves and allows us to estimate the mixing times, for any kind of time-dependent rotational impeller speed tested.

Of course, the model proposed fails to demonstrate that the use of dynamic flow perturbations (time-dependent revolution per minute) contributes to generate a more global chaotic flow which reduces segregated regions and enhances mixing as Tanguy et al. (1998) and Lamberto et al. (2001) have done with CFD applications. The model proposed does not allow to obtain the time-dependent map of the segregated regions. However, our model is quite complementary to CFD applications and very useful since according to us, so far, there was no way to predict by an arrangement of ideal reactors the enhancement of mixing when using time-dependent stirring conditions. In this sense the model proposed succeeds in quantifying quickly the gain in mixing time and energy provided by applying time-dependent RPM.

Moreover, this study has been conducted with a helical ribbon impeller but the approach proposed is not limited to this kind of agitators and can be extended to other mixing systems. It would be even possible to propose a new classification of mixing systems based on their homogenization performances during unsteady stirring and would at last allow to propose new mixers that have an appropriate behaviour when mixing under such operating conditions.

Finally, the mathematical equations of the system are indeed easily tractable which allows to define an optimal control strategy for the torus model. This will be tackled in a future work. The optimal control would be a compromise between the additional energy required to damp down quickly the degree of homogeneity and additional energy required to create dynamic flow perturbations (unsteady rotational speed).

Notation

D	impeller diameter, m
H_c	tank height, m
H_L	liquid height, m
k, α	model parameters (see units in text)
L	impeller height, m
N	impeller rotational speed, rev/s
p	helical ribbon pitch, m
$\dot{Q}$	fluid flow rate, m^3/s
S_1, S_2	moving boundaries for the torus volume, m^2
t	time, s
t_m	mixing time, s
T	tank diameter, m
T_e	sampling period used for estimation, s
V	vessel or torus reactor volume, m^3
V_d	volume of the well-mixed zone for the torus volume, m^3
V_p	volume of the plug flow zone for the torus volume, m^3
w	blade width, m
W_m	mixing work, J
$y(t)$	tracer concentration, kg/m^3

Greek letters

α	proportionality constant, m^3
θ	time-varying delay, s
μ	viscosity of Newtonian fluid, Pa s
ρ	fluid density, kg/m

Appendix A. Derivation of the toroidal reactor model equations

A.1. Space–time for the constant stirred tank zone in the torus loop

Defining $\dot{V}_d^+$ (resp., $\dot{V}_d^-$) as the variation of volume V_d due to the motion of S_1 (resp., S_2) in the torus, variation in

volume V_d with time can be written as

$$\frac{\mathrm{d}[V_d(\dot{Q}(t))]}{\mathrm{d}t} = \dot{V}_d^+ - \dot{V}_d^-. \tag{8}$$

Using notations previously developed, the material balance in the well-mixed zone is

$$\frac{\mathrm{d}[V_d(\dot{Q}(t))y(t)]}{\mathrm{d}t} = (\dot{Q}(t) + \dot{V}_d^+(t))y(t-\theta) - (\dot{Q}(t) + \dot{V}_d^-(t))y(t), \tag{9}$$

where θ is the residence time of the particle leaving the plug flow zone at time t.

Another expression of material balance in the well-mixed zone is

$$\frac{\mathrm{d}[V_d(\dot{Q}(t))y(t)]}{\mathrm{d}t} = V_d(\dot{Q}(t))\frac{\mathrm{d}y(t)}{\mathrm{d}t} + y(t)\frac{\mathrm{d}[V_d(\dot{Q}(t))]}{\mathrm{d}t}, \tag{10}$$

combining Eqs. (8) and (9) with Eq. (10):

$$V_d(\dot{Q}(t))\frac{\mathrm{d}[y(t)]}{\mathrm{d}t} = (\dot{Q}(t) + \dot{V}_d^+)[y(t-\theta) - y(t)]. \tag{11}$$

A.2. Space–time modelling for the plug flow zone in the torus loop

The particle which enters the plug flow zone at the instant $t = t - \theta$ and transported at non-steady flow rate $\dot{Q}$ in a clockwise direction must go through the plug flow volume ahead of it, before leaving at time t. The transport delay θ is defined by the implicit Eq. (12):

$$\int_{t-\theta}^{t} \dot{Q}(\sigma)\,\mathrm{d}\sigma = V_p(\dot{Q}(t-\theta)) - \int_{t-\theta}^{t} \dot{V}_d^+(\sigma)\,\mathrm{d}\sigma. \tag{12}$$

Due to the clockwise flow direction, the plug flow volume ahead of the particle can only decrease during the route. This decrease corresponds to the second right term of Eq. (12).

Appendix B. Material balance in the torus reactor (proof of the theorem)

Since $\dot{V}_d + \dot{V}_p = 0$,

$$\begin{aligned} V_p(t) - V_p(t-\theta) &= \int_{t-\theta}^{t} \dot{V}_p(\sigma)\,\mathrm{d}\sigma \\ &= -\int_{t-\theta}^{t} \dot{V}_d(\sigma)\,\mathrm{d}\sigma \\ &= \int_{t-\theta}^{t} (\dot{V}_d^- - \dot{V}_d^+)\,\mathrm{d}\sigma, \end{aligned}$$

and Eq. (12) can be rewritten as

$$\int_{t-\theta}^{t} \dot{Q}(\sigma)\,\mathrm{d}\sigma = V_p(t) - \int_{t-\theta}^{t} \dot{V}_d^-(\sigma)\,\mathrm{d}\sigma.$$

At time t, the quantity $A(t)$ of the species y inside the reactor is the sum of that in the plug flow and the well-mixed zones,

$$A(t) = V_d(t)y(t) - \int_{plug\ flow} y(t-\theta(z,t))S\,\mathrm{d}z,$$

where S is the constant surface of the torus section and $\theta(z,t)$ is the time delay of a particle whose position in the plug flow zone is z. The abscissa z ranges from 0 to $V_p(t)/S$. The particles which are at position z at time t have entered the plug flow zone at time $t - \theta(z,t)$. These particles had to travel the distance $z - \frac{1}{S}\int_{t-\theta(z,t)}^{t} \dot{V}_d^-(\sigma)\,\mathrm{d}\sigma$ which yields the following relation which in turn generalizes Eq. (12):

$$\int_{t-\theta(z,t)}^{t} \dot{Q}(\sigma)\,\mathrm{d}\sigma = Sz - \int_{t-\theta(z,t)}^{t} \dot{V}_d^-(\sigma)\,\mathrm{d}\sigma.$$

Now let us show that the derivative of $A(t)$ is zero.

Deriving the equation above with respect to t and z, we obtain the useful relations

$$\begin{aligned} &\dot{Q}(t) + \dot{V}_d^-(t) = (\dot{Q}(t-\theta(z,t)) + \dot{V}_d^-(t-\theta(z,t)))\left(1 - \frac{(\partial\theta(t-\theta(z,t),z))}{\partial t}\right), \\ &\frac{\partial\theta(z,t)}{\partial t}(\dot{Q}(t-\theta(z,t)) + \dot{V}_d^-(t-\theta(z,t))) = S. \end{aligned}$$

First we calculate

$$\begin{aligned} &\frac{\mathrm{d}}{\mathrm{d}t}\int_{plug\ flow} y(t-\theta(z,t))S\mathrm{d}z \\ &\quad = \dot{V}_p(t)y(t-\theta) + \int_0^{V_p/S} \dot{y}(t-\theta(z,t)) \times \left(1 - \frac{(\partial\theta(t-\theta(z,t),z))}{\partial t}\right) S\,\mathrm{d}z, \end{aligned}$$

which becomes, using previous equations,

$$\begin{aligned} &\frac{\mathrm{d}}{\mathrm{d}t}\int_{plug\ flow} y(t-\theta(z,t))S\,\mathrm{d}z \\ &\quad = \dot{V}_p(t)y(t-\theta) + \int_0^{V_p/S} \dot{y}(t-\theta(z,t)) \times \frac{\dot{Q}(t) + \dot{V}_d^-(t)}{(\dot{Q}(t-\theta(z,t)) + \dot{V}_d^-(t-\theta(z,t)))} S\,\mathrm{d}z \end{aligned}$$

$$\begin{aligned} &\frac{\mathrm{d}}{\mathrm{d}t}\int_{plug\ flow} y(t-\theta(z,t))S\,\mathrm{d}z \\ &\quad = \dot{V}_p(t)y(t-\theta) + (\dot{Q}(t) + \dot{V}_d^-(t)) \times \int_0^{V_p/S} \dot{y}(t-\theta(z,t))\frac{\partial\theta(z,t)}{\partial z} S\,\mathrm{d}z, \end{aligned}$$

and, integrating the last equation

$$\begin{aligned} &\frac{\mathrm{d}}{\mathrm{d}t}\int_{plug\ flow} y(t-\theta(z,t))S\,\mathrm{d}z \\ &\quad = \dot{V}_p(t)y(t-\theta) + (\dot{Q}(t) + \dot{V}_d^-(t))(y(t) - y(t-\theta(t))). \end{aligned}$$

Replacing in the derivative of $A(t)$ yields

$$\dot{A}(t) = (\dot{Q}+\dot{V}_d^-)y(t-\theta)-(\dot{Q}+\dot{V}_d^-)y(t)+\dot{V}_p(t)y(t-\theta) + (\dot{Q}(t) + \dot{V}_d^-(t))(y(t) - y(t - \theta(t))),$$

$$\dot{A}(t) = (\dot{V}_d^+ - \dot{V}_d^- + \dot{V}_p)y(t - \theta) = 0,$$

which completes the proof.

References

Alvarez-Hernández, M.M., Shinbrot, T., Zalc, J., Muzzio, F.J., 2002. Practical chaotic mixing. Chemical Engineering Science 57, 3749–3753.

Arratia, P.E., Lacombe, J.P., Shinbrot, T., Muzzio, F.J., 2004. Segregated regions in continuous laminar stirred tank reactors. Chemical Engineering Science 59, 1481–1490.

Benkhelifa, H., Legrand, J., Legentilhomme, P., Montillet, A., 2000. Study of the hydrodynamic behaviour of the batch and continuous torus reactor in laminar and turbulent flow regimes by means of tracer methods. Chemical Engineering Science 55, 1871–1882.

Campolo, M., Sbrizzai, F., Soldati, A., 2003. Time-dependent flow structures and Lagrangian mixing in Rushton-impeller baffled-tank reactor. Chemical Engineering Science 58, 1615–1629.

Delaplace, G., Leuliet, J.-C., Relandeau, V., 2000a. Circulation and mixing times for helical ribbon impellers. Review and experiments. Experiments in Fluids 28 (2), 170–182.

Delaplace, G., Torrez, C., André, C., Belaubre, N., Loisel, P., 2000b. Numerical simulation of flow of Newtonian fluids in an agitated vessel equipped with a non standard helical ribbon impeller, Proceedings of 10th European Conference on Mixing, (Delft 2–5 july), (Elsevier Amsterdam): 289–296.

De La Villeon, J., Bertrand, F., Tanguy, P.A., Labrie, R., Bousquet, J., Lebouvier, D., 1998. Numerical investigation of mixing efficiency of helical ribbons. A.I.Ch.E. Journal 44 (4), 972–977.

Dieulot, J.-Y., Richard, J.-P., Tracking control of a nonlinear system with input-dependent delay. IEEE Int. Conf. Decision and Control. CDC 01, Orlando, 2001.

Dieulot, J.-Y., Delaplace, G., Guérin, R., Brienne, J-P., Leuliet, J.-C., 2002. Laminar mixing performances of a stirred tank equipped with helical ribbon agitator subjected to steady and unsteady rotational speed. Transactions of Institution of Chemical Engineers 80 (Part A), 335–344.

Harvey, A.D., Rogers, S.E., 1996. Steady and unsteady computation of impeller stirred tank reactors. A.I.Ch.E. Journal 42, 2701–2712.

Khang, S.J., Levenspiel, O., 1976. New scale-up and design method for stirrer agitated batch mixing vessels. Chemical Engineering Science 31, 569–577.

Lamberto, D.J., Muzzio, F.J., Swanson, P.D., Tonkovich, A.L., 1996. Using time-dependent RPM to enhance mixing in stirred vessels. Chemical Engineering Science 51 (5), 733–741.

Lamberto, D.J., Alvarez, M.M., Muzzio, F.J., 2001. Computational analysis of regular and chaotic mixing in a stirred tank reactor. Chemical Engineering Science 56 (16), 4887–4899.

Metzner, A.B., Taylor, J.S., 1960. Flow patterns in agitated vessels. A.I.Ch.E. Journal 6 (1), 109–114.

Niederkorn, T.C., Ottino, J.M., 1994. Chaotic mixing of shear-thinning fluids. A.I.Ch.E. Journal 40 (11), 1782–1793.

Nomura, T., Uchida, T., Takahashi, K., 1997. Enhancement of mixing by unsteady agitation of an impeller in an agitated vessel. Journal of Chemical Engineering of Japan 30 (5), 875–879.

Ottino, J.M., 1989. The Kinematics of Mixing. Stretching, Chaos and Transport. Cambridge University Press, Cambridge.

Tanguy, P.A., Thibault, F., Brito-De La Fuente, Espinosa Solares, T., Tecante, A., 1998. Mixing performance induced by coaxial flat blade-helical ribbon impellers rotating at different speeds. Chemical Engineering Science 52 (11), 1733–1741.

Tatterson, G.B., 1994. Scale Up and Design of Industrial Mixing Processes. McGraw-Hill, New York.

Yao, W.G., Sato, H., Takahashi, K., Koyama, K., 1998. Mixing performance experiments in impeller stirred tanks subjected to unsteady rotational speeds. Chemical Engineering Science 53 (17), 3031–3043.

Zalc, J.M., Szalai, E.S., Alvarez, M.M., Muzzio, F.J., 2002. Using CFD To Understand Chaotic Mixing in Laminar Stirred Tanks. A.I.Ch.E. Journal 48, 2124–2134.

Zenger, K., Ylinen, R., 1994. Simulation of variable delays in material transport models. Mathematics and Computers in Simulation 37, 57–72.